Materiały Wysokoenergetyczne / High Energy Materials, ***2020***, *12 (2), 29 − 41; DOI 10.22211/matwys/0195*
ISSN 2083-0165

Research paper / Praca doświadczalna

Blast wave energy absorbing systems made using a 3D printing technique – preliminary research
Układy absorbujące energię fali podmuchowej wykonane za pomocą techniki druku 3D – badania wstępne

Karolina Wierzbicka, Józef Paszula*

Military University of Technology, Institute of Chemistry, 2 gen. S. Kaliskiego Street, 00-908 Warsaw, Poland
** E-mail:* jozef.paszula@wat.edu.pl

Abstract: *The study presents the design of blast wave absorbers made using a 3D printing technique. The absorbing properties of these were evaluated by changing the absorbing system's porosity, mass, type and use of additional absorbing materials in a two-layer arrangement. The characteristics of the blast waves generated by a phlegmatized RDX charge for those absorbing systems were measured and the determined parameters compared with the parameters for charges without absorbers. The system showing the best absorbing properties, were selected.*
Streszczenie: *W pracy zaprojektowano i wykonano absorbery fal podmuchowych za pomocą techniki druku 3D. Zdolność tłumienia badano zmieniając: porowatość układów, masę oraz obecność i rodzaj dodatkowego materiału tłumiącego w układach dwuwarstwowych. Zmierzono charakterystyki fal podmuchowych generowanych detonacją ładunku prasowanego heksogenu flegmatyzowanego z osłoną tłumiącą i porównano je z parametrami ładunku nieosłoniętego. Po wyznaczeniu parametrów fal podmuchowych wytypowano absorbery, które charakteryzowały się najlepszymi zdolnościami tłumiącymi.*

Keywords: *blast wave absorbers, 3D printing technique, blast wave overpressure measurements*
Słowa kluczowe: *absorbery fal podmuchowych, druk techniką 3D, pomiar nadciśnienia fal podmuchowych*

1. Introduction

The air blast wave and the unloading waves propagated downstream of the blast wave are one of the main parameters influencing the damage caused by an explosion. The mechanical action of the wave can be destructive to people, buildings and vehicles [1]. To provide efficient protection against a blast wave generated by an explosive, effective absorbing systems must be developed. The main task of such systems is to protect threatened objects and increase safety.

There have been many studies on selecting optimum materials for use in absorbing systems. Systems based on foamed polymers and metallic foams [2-5], multi-layered sandwich structures with different inner core shapes [6-9], grain structures [10-12] and water-based structures [12, 13], have been analysed.

The rapid development of 3D printing techniques has made additive polymer component manufacturing a common and readily available process. Components manufactured using additive techniques tend to be more precise and can be used to make any structure which is labour intensive or almost impossible to manufacture

using conventional techniques.
This study presents results of an analysis of the use of a 3D printing technique to manufacture effective absorbing systems. Single-layer structures with different porosity and mass, and two-layer structures including a 3D printed component with specific porosity and geometry and an additional absorbing material (water, sand, polyurethane foam, shaving foam, non-Newtonian fluid), were analysed.

2. Experimental section

2.1. Specification of materials used

2.1.1. Explosive

Phlegmatized hexogen (6% added wax), manufactured by *Nitro-Chem S.A.*, was used in the tests. Identical, pressed charges with a mass of 75 g, diameter of 30 mm and density of 1.67 g/cm^3 were used in all the tested systems.

2.1.2. Filaments

Filaments were selected based on their density and mechanical properties. After analysing available material data sheets [14, 15], the following filaments were used in the absorbing systems: *Z-ULTRAT* and *Copperfill.* Table 1 shows the main parameters.

Table 1. Filament parameters

Parameter	Filament	
	Copperfill	***Z-ULTRAT***
Company	ColorFabb	Zortrax
Polymer	PLA	ABS
Additional ingredient	approx. 85% copper powder	approx. 3% polycarbonate
Density [g/cm^3]	4.0	1.179
Product density [g/cm^3]	3.0	0.95
Important property	high density	high toughness

The density of the components printed using *Z-ULTRAT* and *Copperfill* filaments was analysed to verify the actual density of the filaments. The density of the end products was lower than that specified by the manufacturer. The determined densities were entered into the software generating the 3D printer code. The mass of the absorbers calculated by the software, the mass calculated at the design stage and the actual mass of the printed components, were similar.

2.2. Absorbers

2.2.1. CAD designs

Following an analysis of the equations in the *Ultimaker Cura* database, a *gyroid* infill pattern was used. The infill is characterized by a spatial change in shape which means that no empty channels are formed along the entire printed component. Figure 1 shows the printed component structure with different porosities. The printed absorbers showed porosities of 50, 25 and 0%.

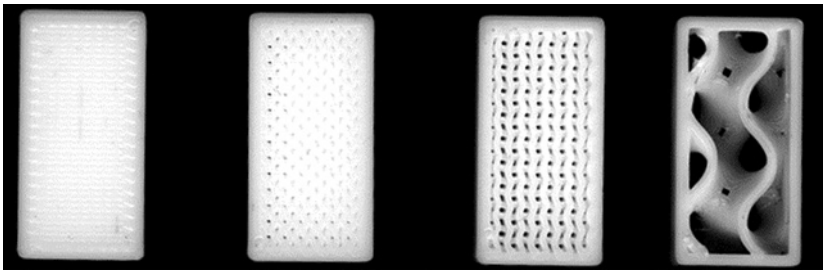

Figure 1. The *gyroid* structure with different porosities: (from left) 90%, 50%, 25%, 0%

The blast wave absorbers were designed using *Autodesk Inventor* software. Three model groups were made:
– Group A: absorbing tubes,
– Group B: absorbing material containers,
– Group C: mixed systems including absorbing tubes and absorbing material containers.

16 different systems were printed. For easy and quick identification, the following labels were used (see Table 2), where the first section (U or M) corresponds to the type of filament used to print the absorber (M – *Copperfill*, U – *Z-Ultrat*). In Groups A and C, the second section corresponds to the thickness of the absorbing tube wall [mm], and the third section corresponds to the porosity of the printout (0, 25 or 50%). The labels in Group B and C also include a section corresponding to the additional blast wave absorbing material:
– CN: non-Newtonian liquid,
– H_2O: water,
– PG: shaving foam,
– PU: polyurethane foam,
– P: sand.

Table 2. System label

No.	Group A	No.	Group B	No.	Group C
1	U-10-0	8	U-CN	13	U-10-0-CN
2	U-10-0.25	9	U-H_2O	14	U-10-0.25-CN
3	U-10-0.5	10	U-PG	15	U-10-0-PU
4	U-20-0.5	11	U-PU	16	U-10-0.25-PU
5	M-10-0	12	U-P		
6	M-6-0.5				
7	M-4.3-0.5				

Figures 2-4 show the dimensions of the designed absorbers, and Tables 3-5 show the dimensions for specific system types. Some dimensions were fixed and were not changed at the design stage for the specific groups of absorbers. The fixed parameters included:
– fuse alignment hole diameter (ϕ_i),
– explosive charge alignment ring diameter (ϕ_{MW}),
– explosive charge height (h),
– absorber height (H),
– explosive distance from the absorber wall (z),
– external wall thickness (x) (Group B and C).

Parameters changed during the tests included:
– absorbing tube thickness (d) (Group A and C), and
– additional absorbing material layer thickness (D) (Group B and C).

The layer thickness is selected to achieve a similar mass of infill material (water, sand, non-Newtonian liquid).

Due to very low foam density (ρ_{PG} = 0.0325°g/cm^3, ρ_{PU} = 0.0517 g/cm^3), the thickness corresponding to that of the water layer was used.

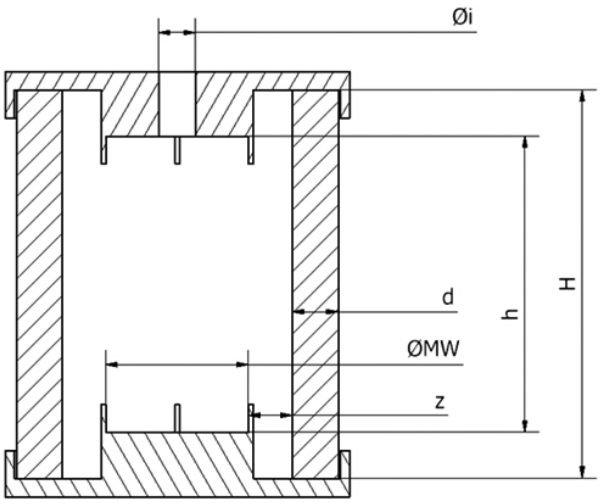

Figure 2. Absorbing system diagram – Group A

Table 3. System dimensions – Group A

Group A	ϕ_i **[mm]**	d **[mm]**	ϕ_{MW} **[mm]**	z **[mm]**	h **[mm]**	H **[mm]**
U-10-0	8.0	10.0	31.0	10.0	64.3	84.3
U-10-0.25						
U-10-0.5						
U-20-0.5		20.0				
M-10-0.5		10.0				
M-6-0.5		6.0				
M-4.3-0.5		4.3				

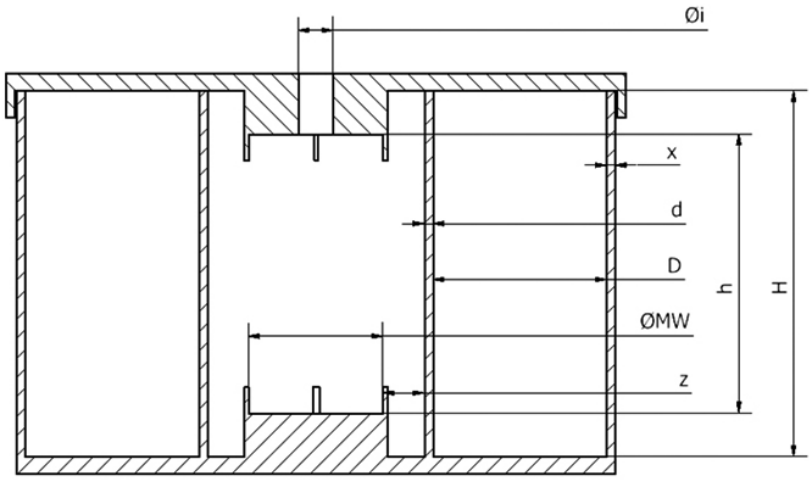

Figure 3. Absorbing system diagram – Group B

Table 4. System dimensions – Group B

Group B	ϕ_i [mm]	d [mm]	ϕ_{MW} [mm]	z [mm]	h [mm]	H [mm]	x [mm]	D [mm]
U-CN	8.0	2.0	31.0	10.0	64.3	84.3	2.0	40.0
U-H_2O								42.7
U-PG								
U-PU								
U-P								30.2

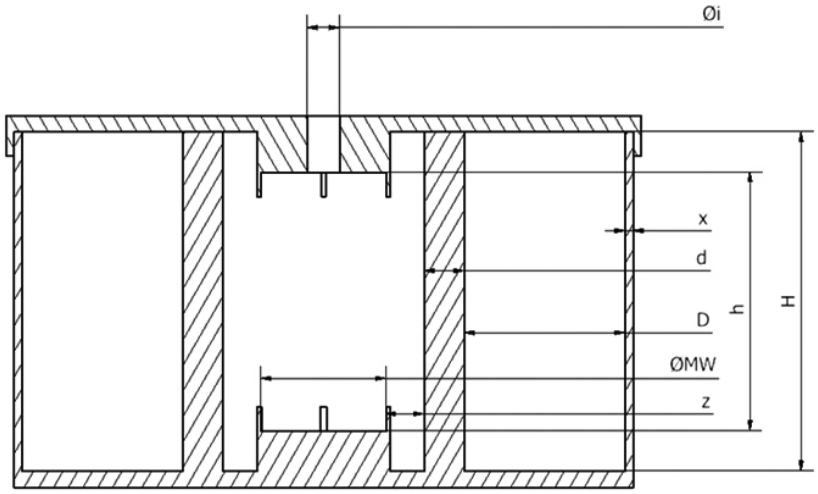

Figure 4. Absorbing system diagram – Group C

Table 5. System dimensions – Group C

Group C	ϕ_i [mm]	d [mm]	ϕ_{MW} [mm]	z [mm]	h [mm]	H [mm]	x [mm]	D [mm]
U-10-0-CN	8.0	10.0	31.0	10.0	63.4	83.4	2.0	40.0
U-10-0.25-CN								
U-10-0-PU								42.7
U-10-0.25-PU								

The absorber mass was a key factor. U-10-0, U-20-0.5 and M-6-0.5 system dimensions were designed to achieve a mass similar to the U-10-0 system (approximately 168 g), despite differences in filament density, geometry and porosity of the absorbers.

2.2.2. Experimental systems used in the tests

For each designed system, cover plates were printed to align the pressed explosive, the fuse and close the system, to limit the scatter of detonation products along the system's axis of symmetry. To minimize the effect of detonation product scatter in the axial directions on the measured blast waves in radial directions of the container, cardboard sand boxes were attached to the cover plates. Fixed layers of sand with similar masses were used with the surface density of the sand always higher than that of the absorber.

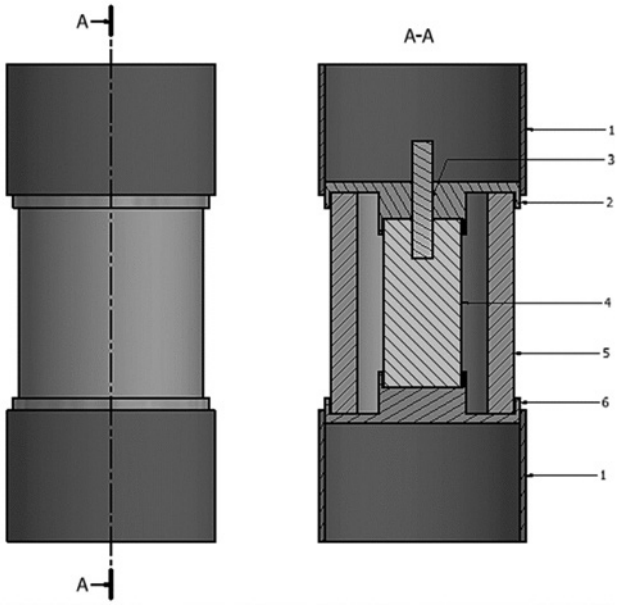

Figure 5. System ready for tests: 1 – cardboard sand box with a 45 mm sand layer and the cardboard cover, 2 – fuse and explosive charge aligning plate, 3 – fuse, 4 – explosive charge, 5 – 3D printed blast wave absorber, 6 – explosive charge aligning plate

2.3. Test system

The pressure generated by the charges was measured using 137A22 and 137B22B Free Field Blast ICP® Pressure sensors. The absorbing system was supported in the blast chamber at the height of piezoelectric sensors (1.5 m above ground) with the sensor surface parallel to the direction of wave propagation (Fig. 6).

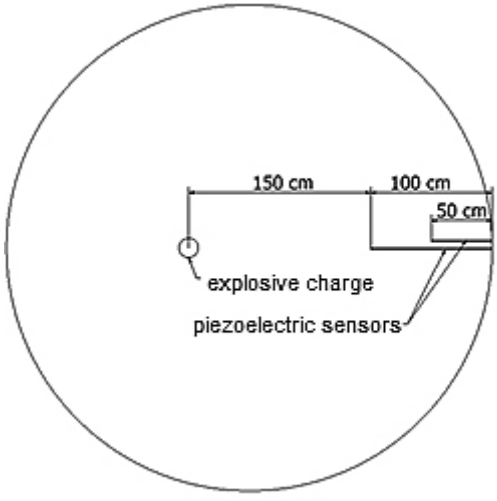

Figure 6. Diagram of test layout in the blast chamber

3. Test results of the absorber's effect on blast wave absorption

3.1. Measurement of pressed phlegmatized hexogen charge parameters

In the first stage, the detonation velocity of the hexogen charges was measured and the characteristics of the blast waves generated by an unobstructed charge, were determined. The detonation velocity was measured using velocity probes and was 8350 m/s. Table 6 shows the characteristics of the blast wave generated by an unobstructed charge.

Table 6. Characteristics of the blast wave generated by an unobstructed RDX

Overpressure [kPa] at a distance of [m]		Impulse [Pa·s] at a distance of [m]		Positive phase duration [ms] at a distance of [m]	
1.5	**2.0**	**1.5**	**2.0**	**1.5**	**2.0**
69.3 ±2.8	37.9 ±1.5	22.8 ±0.9	15.4 ±0.6	0.90 ±0.04	1.10 ±0.04

3.1. Effect of absorber porosity

First, the effect of porosity of the printed systems with predefined *gyroid* pattern infill were evaluated. U-10-0, U-10-0.25 and U-10-0.5 systems were prepared. Blast wave overpressure curves were approximated using a modified Friedlander equation, and the obtained blast wave characteristics are shown in Table 7.

Table 7. The effect of porosity on blast wave absorption (*Z-Ultrat*)

Label	Overpressure [kPa] at a distance of [m]		Impulse [Pa·s] at a distance of [m]		Positive phase duration [ms] at a distance of [m]	
	1.5	**2.0**	**1.5**	**2.0**	**1.5**	**2.0**
U-10-0	36.8 ±1.5	19.1 ±0.8	10.6 ±0.4	7.2 ±0.3	0.78 ±0.03	1.01 ±0.04
	29.6 ±2.5	24.1 ±1.2	11.8 ±2.1	9.9 ±0.4	1.08 ±0.10	1.13 ±0.05
U-10-0.25	47.2 ±1.9	27.8 ±1.1	15.2 ±0.6	11.9 ±0.5	0.88 ±0.04	1.16 ±0.05
U-10-0.5	73.7 ±2.9	38.4 ±1.5	22.9 ±0.9	15.6 ±0.6	0.84 ±0.03	1.10 ±0.04

The test results showed that the U-10-0 system had the greatest effect in lowering blast wave overpressure. To verify these results, an additional test using the selected system was carried out. Figure 7 shows the overpressure *vs.* porosity output. The maximum overpressure results show that the absorbing systems with 0% porosity absorbed blast overpressure at a distance of 1.5 m below the overpressure generated by the unobstructed explosive charge material, measured at a distance of 2.0 m from the explosion centre. The better blast wave absorption by the material with 0% porosity may be due to its highest cohesive forces among the materials and the fact that it may require more work to expand the absorption tube. Absorbing layers with 25 and 50% porosity show low cohesion due to the manufacturing technique used and can easily delaminate and crack, forming layers of fragments as a result of explosion gases. This effect can probably cause a slower dissipation of explosive gas energy and, as a consequence, at a distance of 1.5 m, the parameters are similar to those determined for an unobstructed charge. An additional factor which may cause similar pressures includes disturbances due to impact of fragments on the sensors.

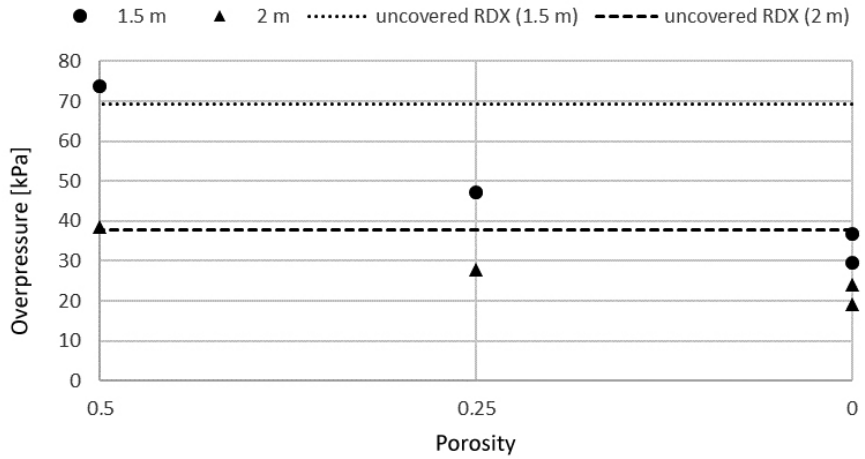

Figure 7. Overpressure *vs.* absorber porosity curve

3.2. Effect of absorber thickness

In the next stage, the effect of absorber thickness with a fixed mass corresponding to the U-10-0 system mass and a porosity corresponding to the U-10-0.5 system (50%) but with twice the thickness, were analysed. A U-20-0.5 absorbing system was prepared. Figure 8 shows an example of overpressure outputs and approximated curves for the test.

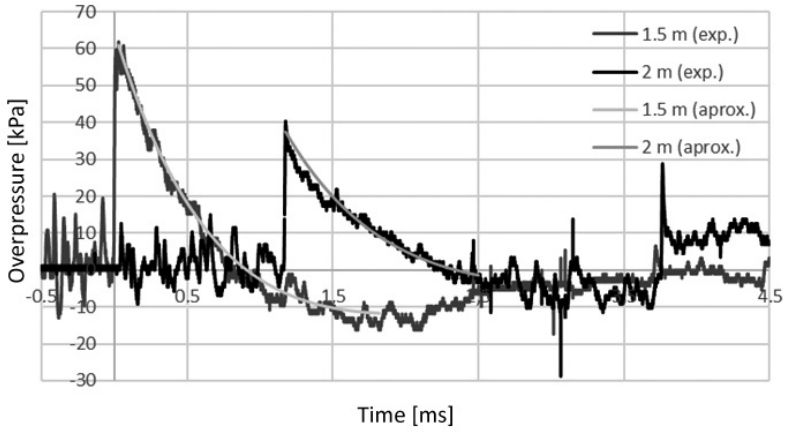

Figure 8. Overpressure *vs.* time outputs for the charge and U-20-0.5 absorber system

Table 8. The effect of mass (geometry) on blast wave absorption (*Z-Ultrat*)

Label	Overpressure [kPa] at a distance of [m]		Impulse [Pa·s] at a distance of [m]		Positive phase duration [ms] at a distance of [m]	
	1.5	2.0	1.5	2.0	1.5	2.0
U-20-0.5	60.9 ±0.6	37.5 ±1.3	20.2 ±0.5	14.3 ±0.2	0.88 ±0.02	1.17 ±0.05

The U-20-0.5 absorber showed a slightly higher absorption than U-10-0.5, however, the increased system mass and its geometry, slightly affect the blast wave absorption parameters. The test results show a significantly

worse absorption compared to the U-10-0 system, indicating that despite the similar mass of the system, 0% porosity in the 3D printed systems using *Z-Ultrat* filaments, shows the highest blast absorption capabilities. Figure 9 shows the overpressure values for systems with different absorbing layer thicknesses and porosities.

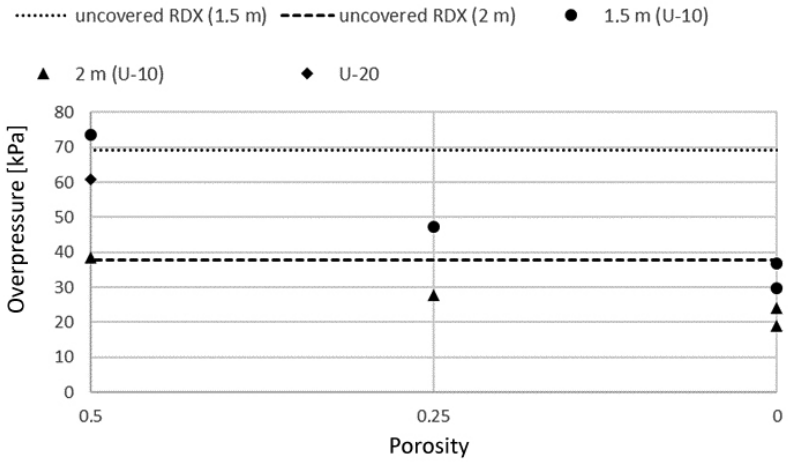

Figure 9. Overpressure vs. absorber porosity and thickness (*Z-Ultrat*) curve

The next stage involved an analysis of the effect of absorber thickness made of *Copperfill* filaments with 50% porosity, on blast wave absorption. The systems with M-6-0.5 (absorber mass similar to that of U-10-0), M-10-0.5 (mass larger than U-10-0) and M-4.3-0.5 (mass smaller than U-10-0), absorbers were prepared.

Table 9. The effect of mass (thickness) on blast wave absorption (*Copperfill*)

Label	Overpressure [kPa] at a distance of [m]		Impulse [Pa·s] at a distance of [m]		Positive phase duration [ms] at a distance of [m]	
	1.5	2.0	1.5	2.0	1.5	2.0
M-6-0.5	63.2 ±1.7	35.9 ±0.4	22.0 ±0.2	15.2 ±0.1	0.95 ±0.02	1.15 ±0.01
M-10-0.5	68.8 ±3.2	33.2 ±1.7	22.5 ±0.3	14.3 ±0.2	0.89 ±0.03	1.18 ±0.05
M-4.3-0.5	69.4 ±4.7	37.1 ±1.0	23.6 ±0.6	15.4 ±0.4	0.97 ±0.04	1.13 ±0.02

Tests of absorbers made of *Copperfill* filaments, showed that they did not demonstrate any blast wave absorption capabilities. Figure 10 shows the test results. The lack of absorbing properties may result from low tensile strength. In the case of tube expansion, the detonation products do not perform significant work and, as a result, the amplitude of the blast wave is not decreased.

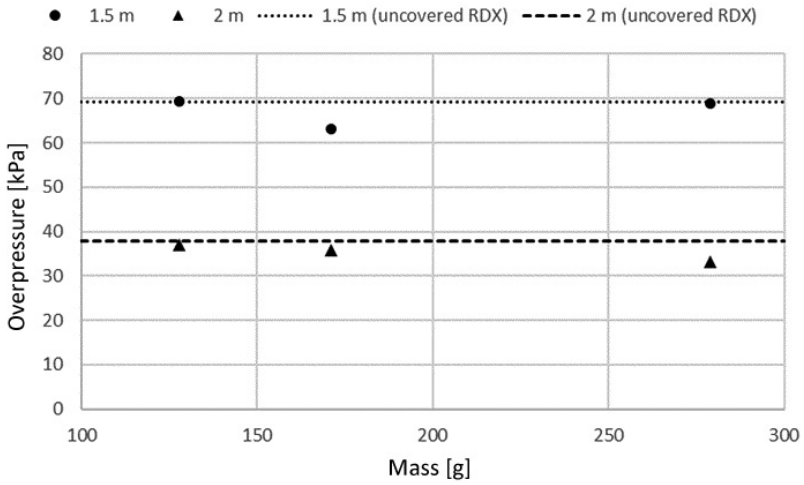

Figure 10. The overpressure *vs.* absorber (*Copperfill*) thickness curve

3.3. Effect of absorbent type

After selecting the best 3D-printed absorber (U-10-0), absorbing properties of materials other than those used in the 3D printing techniques, were evaluated. The following systems were prepared: U-CN, U-H_2O, U-PU, U-PG and U-P. Table 10 and Figure 11 show the results for these systems.

Table 10. The effect of absorber type on blast wave absorption

Label	Overpressure [kPa] at a distance of [m]		Impulse [Pa·s] at a distance of [m]		Positive phase duration [ms] at a distance of [m]	
	1.5	2.0	1.5	2.0	1.5	2.0
U-CN	49.7 ±1.1	26.5 ±1.3	23.62 ±0.06	14.9 ±0.5	1.19 ±0.01	1.48 ±0.02
U-PU	58.8 ±6.2	32.5 ±4.3	18.8 ±1.5	13.6 ±0.4	0.85 ±0.08	1.16 ±0.01
U-PG	47.1 ±1.9	28.6 ±0.8	17.1 ±0.3	11.3 ±0.2	0.91 ±0.04	1.00 ±0.04
U-P	43.9 ±0.6	26.6 ±1.2	20.9 ±1.2	13.7 ±1.0	1.17 ±0.10	1.34 ±0.02

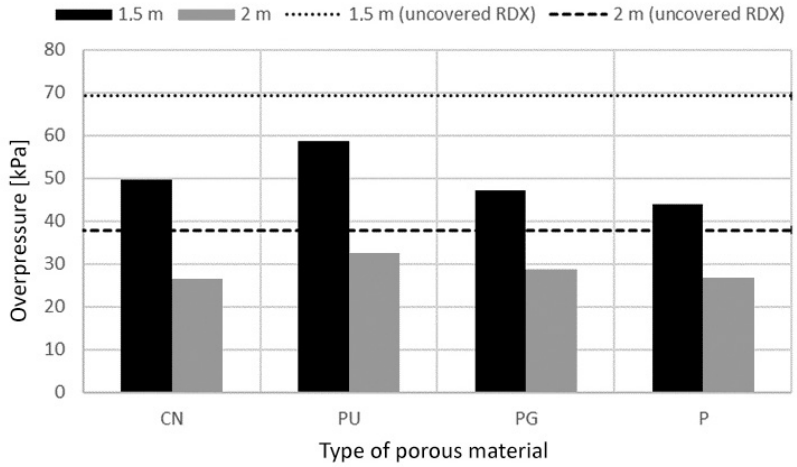

Figure 11. Overpressure *vs.* absorbing material type output

The tests showed that sand is the best absorbing material. Unfortunately, during detonation, the sand grains in the absorber impacted the sensors and generated significant interferences in the output. Despite measuring a relatively low blast wave overpressure, due to low density (ρ_{PG} = 0.0325 g/cm^3), low durability and a relatively short decomposition time, the system including the shaving foam was eliminated from the tests. Two-layered systems including a polyurethane foam (ρ_{PU} = 0.0517 g/cm^3) and a non-Newtonian liquid (mixture of water and potato starch in 5:6 ratio), were used in the tests.

3.4. Two-layer systems

The following systems were tested: U-10-0-CN, U-10-0,25-CN, U-10-0-PU and U-10-0.25-PU. U-10-0.25-CN and U-10-0-PU are the best two-layer systems. Table 11 shows the resulting measurements of the blast wave characteristics. The outputs shown in Figures 12 and 13 were compared with a system from Group B (container and absorber) with a 100% porosity of the absorbing tube.

Table 11. The effect of a two-layer system on blast wave absorption

Label	Overpressure [kPa] at a distance of [m]		Impulse [Pa·s] at a distance of [m]		Positive phase duration [ms] at a distance of [m]	
	1.5	2.0	1.5	2.0	1.5	2.0
U-10-0-CN	46.7 ±2.7	29.8 ±1.2	23.68 ±0.07	16.3 ±1.0	1.25 ±0.12	1.37 ±0.03
U-10-0.25-CN	40.6 ±0.7	24.3 ±0.6	18.5 ±1.7	11.9 ±0.5	1.11 ±0.09	1.25 ±0.04
U-10-0-PU	41.0 ±1.7	22.8 ±1.0	14.2 ±0.9	11.0 ±1.0	0.94 ±0.02	1.31 ±0.05
U-10-0.25-PU	47.6 ±0.9	35.7 ±4.2	14.0 ±0.6	13.5 ±1.2	1.04 ±0.24	1.21 ±0.03

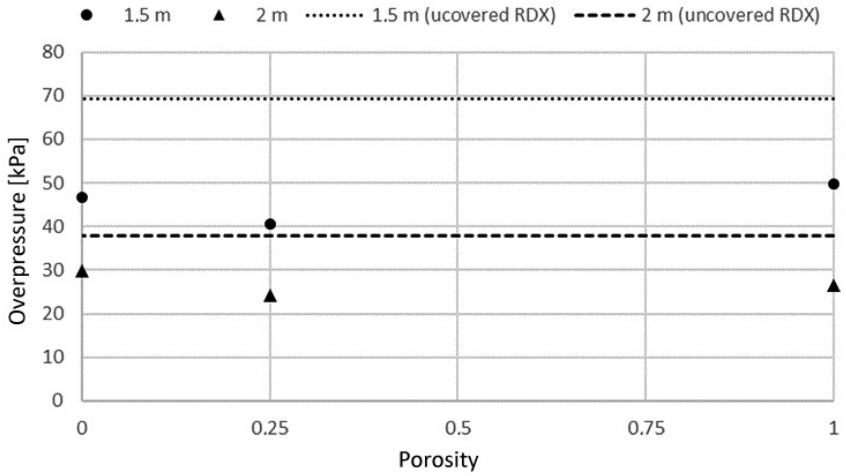

Figure 12. Overpressure *vs.* porosity curve for the systems including a non-Newtonian liquid

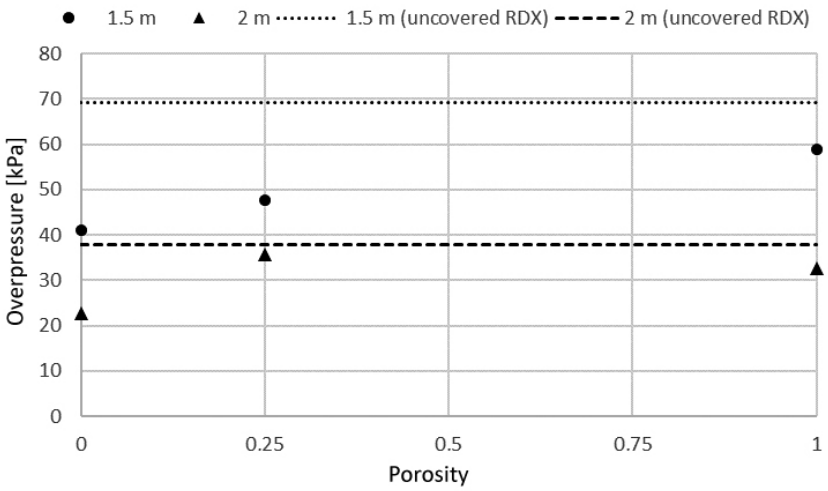

Figure 13. Overpressure *vs.* porosity output for systems incorporating a polyurethane foam

4. Conclusions

Comparing the characteristics of the blast waves for the tested systems shows that most of those made using *Z-Ultrat* filament absorbed the blast wave generated by the hexogen charge, to a certain degree. The overpressure measured for the U-10-0 system was approx. 43% (at 1.5 m) and approx. 64% (at 2.0 m) of the overpressure generated by an unobstructed charge. The other single-layer systems reduced the overpressure by no more than 63% (at 1.5 m) and 70% at (2.0 m).

The systems made with *Copperfill* filament, due to their the low tensile strength, did not show any absorbing capabilities. This phenomenon, despite the high filament density, is caused by a filament content of 85% powdered copper and 15% polymer, bonding the metal. During the interaction with the blast wave following detonation, instead of retaining the gaseous detonation products, the absorbers were damaged much faster than those made of filaments containing 100% polymer.

Fragments found in the blast chamber were caused by cracking and delamination of the printed components indicating that the less porous absorbers, in which the filament layers are better bonded together, are less susceptible to damage.

The absorbing system showing significant blast absorption capabilities (approx. 57% at 1.5 m and approx. 36% at 2.0 m) from Group A, is the U-10-0 system showing the highest tensile strength due to a 0% porosity. Its structure is the most uniform and so the explosion gases performed the most work in order to propel the absorbing layers.

An absorber with 25% porosity was selected for the two-layer system tests to verify if the additional absorbing material would improve their absorbing capabilities.

The two-layer systems, including a non-Newtonian liquid/absorber with 25% porosity and a polyurethane foam/absorber with 0% porosity, showed the highest absorbing capabilities of the blast overpressure in their group (Group C). For the U-10-0.25-CN system, this was 59% (at 1.5 m) and 64% (at 2.0 m), whereas for the U-10-0-PU system, it was 59% (at 1.5 m) and 60% (at 2.0 m).

The blast wave absorbers, manufactured using a 3D printing technique and a predefined infill pattern, did not function as intended. More complex infill patterns need to be designed to provide systems with high blast wave absorbing capabilities.

References

[1] Cudziło S., Maranda A., Nowaczewski J., Trębiński R., Trzciński W.A. *Military Expolosives.* (in Polish) Częstochowa: Wyd. Wydziału Metalurgii i Inżynierii Materiałowej Politechniki Częstochowskiej, **2000.**

[2] Komissarov P.V., Borisov A.A., Sokolov G.N., Lavrov V.V. Rigid Polyurethane Foam as an Efficient Material for Shock Wave Attenuation. *J. Phys. Conf. Ser.* **2016**, *751*(1), 012020.

[3] Woodfin R.L. *Using Rigid Polyurethane Foams (RPF) for Explosive Blast Energy Absorption in Applications Such as Anti-Terrorist Defences.* Sandia Report SAND2000-0958, Sandia National Laboratories, **2000**.

[4] Yu Ch-J., Banhart J. *Mechanical Properties of Metallic Foams. h*ttps://www.helmholtz-berlin.de/media/media/spezial/people/banhart/html/B-Conferences/b020_yu1998.pdf [retrieved 20.05.**2020**].

[5] Shim Ch., Yun N., Yu R., Byun D. Mitigation of Blast Effects on Protective Structures by Aluminium Foam Panels. *J. Met.* **2012**, *2*: 170-177.

[6] Mullin M.J., O'Toole B.J. Simulation of Energy Absorbing Materials in Blast Loaded Structures. *8th Int. LS-DYNA Users Conf.*, Las Vegas, Nevada, **2004**.

[7] Ngoc San Ha, Lu G., Xiang X. Energy Absorption of Bio-Inspired Honeycomb Sandwich Panel. *J. Mater. Sci.* **2019**, *54*: 6286-6300.

[8] Matsagar V.A. Comparative Performance Composite Sandwich Panels and Non-Composite Panels under Blast Loading. *Mater. Struct.* **2016**, *49*: 611-629.

[9] Ren L., Ma H., Shen Z., Wang Y., Zhao K. Blast Resistance of Water-Backed Metallic Sandwich Panels Subjected to Underwater Explosion. *Int. J. Impact Eng.* **2019**, *129:* 1-11.

[10] Yu X., Chen L., Fang Q., Chen W. Stress Attenuation and Energy Absorption of the Coral Sand with Different Particle Sizes under Impacts. *Proceedings* **2018**, *2*: 545/1-7.

[11] Yu X., Chen L., Fang Q. Experimental Study on the Attenuation of Stress Wave in Coral Sand. *Chin. J. Rock Mech. Eng.* **2018**, *37:*1520-1529.

[12] Homae T., Sugiyama Y., Wakabayashi K., Matsumura T., Nakayama Y. Water and Sand for Blast Pressure Mitigation Around a Subsurface Magazine. *Sci. Technol. Energ. Mater.* **2016**, *77*: 18-21

[13] Homae T., Wakabayashi K., Matsumura T., Nakayama Y. Blast Pressure Mitigation by Surface Explosion Using Water in a Walled Container. *J. Mech. Eng. Autom.* **2015**, *5*: 317-324.

[14] https://cdn-3d.niceshops.com/upload/file/TDS-copperFill-en[0].pdf [retrevied 16.06.**2020**].

[15] https://cf.zortrax.com/wp-content/uploads/2019/01/Z-ULTRAT_Technical_Data_Sheet_pl.pdf [retrevied 16.06.**2020**].

Received: June 01, 2020
Revised: November 3, 2020
Published first time online: November 25, 2020